Analytical Solution for Bending Steel Concrete Composite Plates considering the Shear Deformation Effect

Dao Ngoc Tien
Hanoi Architectural University, Vietnam
tiendn@hau.edu.vn

Nguyen Xuan Tung
University of Transport and Communications, Ha Noi, Vietnam
ngxuantung@utc.edu.vn

Nguyen Ngoc Lam
University of Transport and Communications, Ha Noi, Vietnam
nngoclamkc@utc.edu.vn (corresponding author)

Received: 11 May 2024 | Revised: 25 June 2024 | Accepted: 3 July 2024

 DOI: https://doi.org/10.48084/etasr.7801

ABSTRACT

This paper deals with an analytical approach to the static behavior of Steel Concrete Composite (SCC) slabs. The Classical Plate Theory (CPT) and Refined Plate Theory (RPT) are considered when constructing governing equations describing the behavior of steel concrete plates. The displacement fields are represented by trigonometric series to find the exact solution by applying Navier's approach. Various numerical examples have been compared with the considered ones showing their high accuracy. The influence of plate parameters such as the thickness of steel and concrete layers on displacement was investigated in detail.

Keywords-Steel Concrete Composite (SCC) plates; analytical solution; refined plate

I. INTRODUCTION

Plate structures have been widely used in civil and mechanical engineering [1-10]. The plate can be manufactured from steel, wood, composite materials, or reinforced concrete. Composite structures, such as bridge decks or floor slabs, combine steel and concrete to leverage the strengths of both materials. Authors in [11] proposed a model of shear connection in the form of discrete points at the actual positions of studs to study the behavior of concrete-steel composite beams. Recently, Ultra-High-Performance Concrete (UHPC) has been deployed to improve the load-carrying capacity of deck slabs, such as the Thang Long (Vietnam) bridge improvement bridge deck project [12]. Authors in [13] implemented Abaqus software to investigate the bond between normal concrete and Ultra-High-Performance Fiber-Reinforced Concrete. Authors in [14] studied the test results of the flexural behavior of prestressed textile-reinforced concrete plates. In [15], the influence of size on the fracture characteristics of Ultra-High-Performance Fiber-Reinforced Concrete was examined.

There is a lack of theoretical studies on the calculation of beams or plates related to steel, concrete, or composite materials. However, analytical and numerical methods have been proposed and applied for plate structures. Authors in [16] approximated the displacement fields following the Navier approach to determine the vibrational response of functionally graded plates. Authors in [17] developed a finite element method utilizing the phase field and third-order shear deformation theory to study the free vibration of cracked plates with varying thickness. They adopted an approach similar to [18], but with the latter combining the edge-based smoothed finite element method and tensorial components triangular element method for the dynamics of sandwich plates. Authors in [19] developed a finite element analysis for continuous sandwich beams subjected to vehicles. Authors in [20] employed the finite element software LS-DYNA to study the penetration of Steel Plate-Reinforced Concrete (SC) walls by projectiles. Authors in [21] carried out experiments on steel plate-strengthened reinforced concrete slabs under dynamic loading to investigate their dynamic behavior. Authors in [22] used a quasi-static loading test to examine the failure of steel-concrete-steel sandwich slabs with bi-directional corrugated-strip connectors. Authors in [23] employed an experimental study on the tensile behavior of SCC plates considering flexural and shear with six full-scale specimens. Despite the

extensive research that has been carried out on panels, there is a deficiency in the number of studies that have deployed analytical methods to investigate SCC panels. This study uses the CPT and the RPT approaches to derive the governing equations for SCC plates and to identify analytical methods for solving them.

II. GOVERNING EQUATION OF HIGH-ORDER SCC PLATES

The SCC plate considered along with its coordinate system are illustrated in Figure 1.

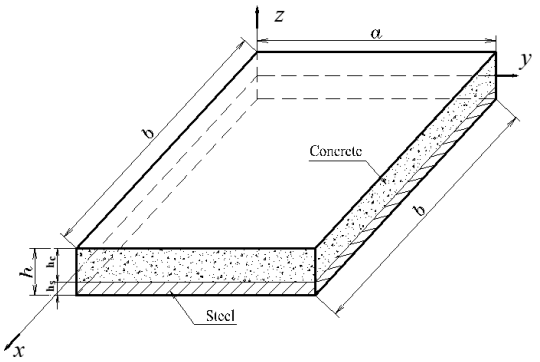

Fig. 1. The Geometry of plate.

The displacement fields at an arbitrary point (*x, y, z*) in the plate are performed using the classical plate theory:

$$\begin{aligned} U(x,y,z,t) &= u(x,y,z,t) - z\frac{\partial w_b}{\partial x} \\ V(x,y,z,t) &= v(x,y,z,t) - z\frac{\partial w_b}{\partial y} \\ W(x,y,z,t) &= w_b(x,y,t) \end{aligned} \quad (1)$$

where u, v, w_b, w_s, are the displacement components on the mid-plane. The steel and concrete are tightly bonded and calculated as a two-layer composite plate. The CPT does not consider shear deformation, which presents a limitation when analysing thick plates. In this study, shear deformation of SCC plates is addressed using an RPT [24]:

$$\begin{aligned} U(x,y,z,t) &= u(x,y,z,t) - z\frac{\partial w_b}{\partial x} + z\left[\frac{1}{4} - \frac{5z^2}{3h^2}\right]\frac{\partial w_s}{\partial x} \\ V(x,y,z,t) &= v(x,y,z,t) - z\frac{\partial w_b}{\partial y} + z\left[\frac{1}{4} - \frac{5z^2}{3h^2}\right]\frac{\partial w_s}{\partial y} \\ W(x,y,z,t) &= w_b(x,y,t) + w_s(x,y,t) \end{aligned} \quad (2)$$

The deformations obtained from the displacements in (1) are:

$$\begin{Bmatrix} \varepsilon_{xx} \\ \varepsilon_{yy} \\ \gamma_{xy} \\ \gamma_{xz} \\ \gamma_{yz} \end{Bmatrix} = \begin{Bmatrix} \frac{\partial u}{\partial x} \\ \frac{\partial v}{\partial y} \\ \frac{\partial u}{\partial y} + \frac{\partial v}{\partial x} \\ \frac{\partial u}{\partial z} + \frac{\partial w}{\partial x} \\ \frac{\partial v}{\partial z} + \frac{\partial w}{\partial y} \end{Bmatrix} \quad (3)$$

or:

$$\begin{Bmatrix} \varepsilon_x \\ \varepsilon_y \\ \gamma_{xy} \end{Bmatrix} = \begin{Bmatrix} \varepsilon_x^0 \\ \varepsilon_y^0 \\ \gamma_{xy}^0 \end{Bmatrix} + \begin{Bmatrix} \kappa_x^b \\ \kappa_y^b \\ \kappa_{xy}^b \end{Bmatrix} + \hat{f}\begin{Bmatrix} \kappa_x^s \\ \kappa_y^s \\ \kappa_{xy}^s \end{Bmatrix},$$

$$\begin{Bmatrix} \gamma_{yz} \\ \gamma_{xz} \end{Bmatrix} = \hat{g}\begin{Bmatrix} \gamma_{yz}^s \\ \gamma_{xz}^s \end{Bmatrix} \quad (4)$$

where:

$$\begin{Bmatrix} \varepsilon_x^0 \\ \varepsilon_y^0 \\ \gamma_{xy}^0 \end{Bmatrix} = \begin{Bmatrix} \frac{\partial u}{\partial x} \\ \frac{\partial v}{\partial y} \\ \frac{\partial u}{\partial y} + \frac{\partial v}{\partial x} \end{Bmatrix}, \begin{Bmatrix} \gamma_{yz}^s \\ \gamma_{xz}^s \end{Bmatrix} = \begin{Bmatrix} \frac{\partial w_s}{\partial y} \\ \frac{\partial w_s}{\partial x} \end{Bmatrix},$$

$$\begin{Bmatrix} \kappa_x^b \\ \kappa_y^b \\ \kappa_{xy}^b \end{Bmatrix} = \begin{Bmatrix} -\frac{\partial^2 w_b}{\partial x^2} \\ -\frac{\partial^2 w_b}{\partial y^2} \\ -2\frac{\partial^2 w_b}{\partial x \partial y} \end{Bmatrix}, \begin{Bmatrix} \kappa_x^s \\ \kappa_y^s \\ \kappa_{xy}^s \end{Bmatrix} = \begin{Bmatrix} -\frac{\partial^2 w_s}{\partial x^2} \\ -\frac{\partial^2 w_s}{\partial y^2} \\ -2\frac{\partial^2 s}{\partial x \partial y} \end{Bmatrix},$$

$\hat{f}(z) = -z\left[\frac{1}{4} - \frac{5z^2}{3h^2}\right]$, and $\hat{g}(z) = \frac{5}{4} - \frac{5z^2}{3h^2}$.

The linear constitutive relations of plates for steel can be written as:

$$\begin{Bmatrix} \sigma_x \\ \sigma_y \\ \sigma_{yz} \\ \sigma_{xz} \\ \sigma_{xy} \end{Bmatrix} = \begin{bmatrix} Q_{11}^s & Q_{12}^s & 0 & 0 & 0 \\ Q_{12}^s & Q_{22}^s & 0 & 0 & 0 \\ 0 & 0 & Q_{44}^s & 0 & 0 \\ 0 & 0 & 0 & Q_{55}^s & 0 \\ 0 & 0 & 0 & 0 & Q_{66}^s \end{bmatrix} \begin{Bmatrix} \varepsilon_x \\ \varepsilon_y \\ \gamma_{yz} \\ \gamma_{xz} \\ \gamma_{xy} \end{Bmatrix} \quad (5)$$

and for concrete:

$$\begin{Bmatrix} \sigma_x \\ \sigma_y \\ \sigma_{yz} \\ \sigma_{xz} \\ \sigma_{xy} \end{Bmatrix} = \begin{bmatrix} Q_{11}^c & Q_{12}^c & 0 & 0 & 0 \\ Q_{12}^c & Q_{22}^c & 0 & 0 & 0 \\ 0 & 0 & Q_{44}^c & 0 & 0 \\ 0 & 0 & 0 & Q_{55}^c & 0 \\ 0 & 0 & 0 & 0 & Q_{66}^c \end{bmatrix} \begin{Bmatrix} \varepsilon_x \\ \varepsilon_y \\ \gamma_{yz} \\ \gamma_{xz} \\ \gamma_{xy} \end{Bmatrix} \quad (6)$$

Regarding the classical plate, its strain energy can be rewritten following the force and moment resultants of the plates:

$$\Pi = \frac{1}{2}\int_A \begin{bmatrix} M_x^b\kappa_x^b + M_y^b\kappa_y^b + M_{xy}^b\kappa_{xy}^b + \\ N_x\varepsilon_x^0 + N_y\varepsilon_y^0 \end{bmatrix} dx\,dy \quad (7)$$

and for the refined plate:

$$\Pi = \frac{1}{2}\int_A \begin{bmatrix} M_x^b\kappa_x^b + M_y^b\kappa_y^b + M_{xy}^b\kappa_{xy}^b + \\ M_x^s\kappa_x^s + M_y^s\kappa_y^s + M_{xy}^s\kappa_{xy}^s + \\ N_x\varepsilon_x^0 + N_y\varepsilon_y^0 + N_{xy}\gamma_{xy}^0 + \\ Q_x\gamma_{xz}^s + Q_y\gamma_{yz}^s \end{bmatrix} dx\,dy \quad (8)$$

where:

$$[N] = \begin{Bmatrix} N_x \\ N_y \\ N_{xy} \end{Bmatrix} = \int_{-h/2}^{h/2} \begin{Bmatrix} \sigma_x \\ \sigma_y \\ \sigma_{xy} \end{Bmatrix} dz,$$

$$[M^b] = \begin{Bmatrix} M_x^b \\ M_y^b \\ M_{xy}^b \end{Bmatrix} = \int_{-h/2}^{h/2} z \begin{Bmatrix} \sigma_x \\ \sigma_y \\ \sigma_{xy} \end{Bmatrix} dz,$$

$$[M^s] = \begin{Bmatrix} M_x^s \\ M_y^s \\ M_{xy}^s \end{Bmatrix} = \int_{-h/2}^{h/2} \hat{f} \begin{Bmatrix} \sigma_x \\ \sigma_y \\ \sigma_{xy} \end{Bmatrix} dz,$$

and $\begin{Bmatrix} Q_x \\ Q_y \end{Bmatrix} = \int_{-h/2}^{h/2} \hat{g} \begin{Bmatrix} \sigma_{xz} \\ \sigma_{yz} \end{Bmatrix} dz.$

The governing equation for the refined plate is obtained by employing the principle of virtual work:

$$\begin{gathered} \frac{\partial N_x}{\partial x} + \frac{\partial N_{xy}}{\partial y} = 0 \\ \frac{\partial N_{xy}}{\partial x} + \frac{\partial N_y}{\partial y} = 0 \\ \frac{\partial^2 M_x^b}{\partial x^2} + 2\frac{\partial^2 M_{xy}^b}{\partial x \partial y} + \frac{\partial^2 M_y^b}{\partial y^2} + q = 0 \\ \frac{\partial^2 M_x^s}{\partial x^2} + 2\frac{\partial^2 M_{xy}^s}{\partial x \partial y} + \frac{\partial^2 M_y^s}{\partial y^2} + \frac{\partial Q_{xz}}{\partial x} + \frac{\partial Q_{yz}}{\partial y} + q = 0 \end{gathered} \quad (9)$$

III. ANALYTICAL SOLUTION

This study only considers simply supported rectangular plates. The boundary conditions for different types of plates are:

Classical plate:

$$\begin{gathered} v = w_b = \frac{\partial w_b}{\partial y} = N_x = M_x^b = 0 \text{ at } x = 0, a \\ u = w_b = \frac{\partial w_b}{\partial x} = N_y = M_y^b = 0 \text{ at } y = 0, b \end{gathered} \quad (10)$$

Refined plate:

$$\begin{gathered} v = w_b = w_s = \frac{\partial w_b}{\partial y} = \frac{\partial w_s}{\partial y} = N_x = \\ M_x^b = M_x^s = 0 \text{ at } x = 0, a \\ u = w_b = w_s = \frac{\partial w_b}{\partial x} = \frac{\partial w_s}{\partial x} = N_y = \\ M_y^b = M_y^s = 0 \text{ at } y = 0, b \end{gathered} \quad (11)$$

The displacement fields are therefore presented as sinusoidal functions:

$$\begin{gathered} u(x,y,t) = \sum_{n=1}^{\infty} \sum_{m=1}^{\infty} U_{mn}(t) cos\alpha x \, sin\beta y \\ v(x,y,t) = \sum_{n=1}^{\infty} \sum_{m=1}^{\infty} V_{mn}(t) sin\alpha x \, cos\beta y \\ w_b(x,y,t) = \sum_{n=1}^{\infty} \sum_{m=1}^{\infty} W_{bmn}(t) sin\alpha x \, sin\beta y \\ w_s(x,y,t) = \sum_{n=1}^{\infty} \sum_{m=1}^{\infty} W_{smn}(t) sin\alpha x \, sin\beta y \end{gathered} \quad (12)$$

where: $\alpha = \frac{m\pi}{a}$ and $\beta = \frac{n\pi}{b}$.

The solution can be found by applying the Navier approach [25].

For the classical plate:

$$\begin{bmatrix} s_{11} & s_{12} & s_{13} \\ s_{12} & s_{22} & s_{23} \\ s_{13} & s_{23} & s_{33} \end{bmatrix} \begin{Bmatrix} U_{mn} \\ V_{mn} \\ W_{bmn} \end{Bmatrix} = \begin{Bmatrix} 0 \\ 0 \\ F_{mn} \end{Bmatrix} \quad (13)$$

For the refined plate:

$$\begin{bmatrix} s_{11} & s_{12} & s_{13} & s_{14} \\ s_{12} & s_{22} & s_{23} & s_{24} \\ s_{13} & s_{23} & s_{33} & s_{34} \\ s_{14} & s_{24} & s_{34} & s_{44} \end{bmatrix} \begin{Bmatrix} U_{mn} \\ V_{mn} \\ W_{bmn} \\ W_{smn} \end{Bmatrix} = \begin{Bmatrix} 0 \\ 0 \\ F_{mn} \\ F_{mn} \end{Bmatrix} \quad (14)$$

where:

$$F_{mn} = \frac{4}{ab} \int_0^b \int_0^a q \, sin\,\alpha x \, sin\,\beta y \, dxdy.$$

IV. NUMERICAL EXAMPLES

1) Example 1: Validation

A rectangular SCC plate is positioned on single supported axial bars. The dimensions of the plate are a=2 m, b=2 m, the thickness ranges from 8 cm to 15 cm. The SCC plate is subjected to the uniform load of $q_0 = 50\ \text{kN/m}^2$. The normalized stresses $\bar{\sigma}_x, \bar{\sigma}_y$ are defined as:

$$\begin{gathered} \bar{\sigma}_x = \sigma_x \left(\frac{a}{2}, \frac{b}{2}, \pm\frac{h}{2}\right) / q_0 \\ \bar{\sigma}_y = \sigma_y \left(\frac{a}{2}, \frac{b}{2}, \pm\frac{h}{2}\right) / q_0 \end{gathered} \quad (15)$$

The plate is placed on two simple supports and the two edges of the plate rest on tension bars, which are 8 cm thick. The example results exhibited in Tables I-IV indicate the displacements and normalized stresses calculated by the CPT and the RPT. Tables II-IV clearly show the effect of plate thickness on displacement and stress, with a significant reduction in displacement as the plate thickness is increased. In addition, as the plate thickness is augmented, the effect of shear deformation becomes more pronounced, resulting in an increase in the plate displacement.

TABLE I. MATERIAL PROPERTIES

Materials	Elastic modulus (GPa)	Poisson's ratio
Concrete	30	0.25
Steel	200	0.3

TABLE II. DEFLECTION IN THE CENTER OF PLATE

Thickness of plate h (cm)	Displacement (mm)		Error (%)
	RPT	CPT	
8	1.2028	1.17	2.80
10	0.6475	0.6186	4.67
12	0.3958	0.3703	6.89
15	0.2205	0.199	10.80

TABLE III. THE NORMALIZED STRESS AT TOP IN THE CENTER OF PLATE

Thickness of plate h (cm)	Normalized stress $\bar{\sigma}_x\left(\frac{a}{2}, \frac{b}{2}, \frac{h}{2}\right)$		Error (%)
	RPT	CPT	
8	119.75	118.84	0.77
10	77.61	76.62	1.29
12	54.85	53.79	1.97
15	36.2	35.09	3.16

TABLE IV. THE NORMALIZED STRESS AT BOTTOM IN THE CENTER OF PLATE

Thickness of plate h (cm)	**Normalized stress** $\sigma_x\left(\frac{a}{2},\frac{b}{2},-\frac{h}{2}\right)$		**Error (%)**
	RPT	CPT	
8	372.24	365.6	1.82
10	262.79	255.4	2.89
12	200.22	192.35	4.09
15	145.07	136.77	6.07

2) Example 2

In this example, a rectangular steel UHPC composite plate is considered, which has the following dimensions and material properties: a = 2 m, b = 3 m, modulus of elasticity and Poisson's ratio UHPC equal to 40 GPa, and 0.25, respectively, while for steel these values are 200 GPa, and 0.3, with a uniformly distributed load of 5.104 N/m². The results of the steel UHPC composite plate displacements are illustrated in Figure 2. The findings of the calculations of the displacements and stresses for three different steel plate thicknesses are presented in Figures 3-5.

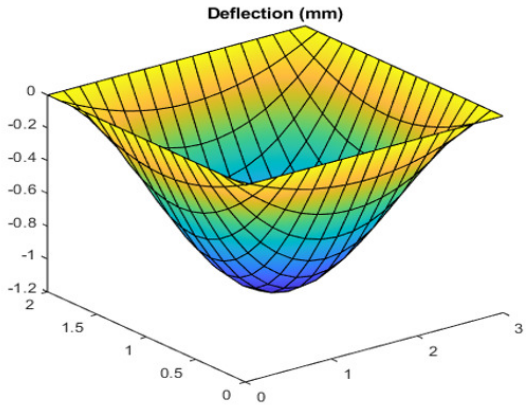

Fig. 2. Displacement of plates with h=10 cm, h_s=16 mm.

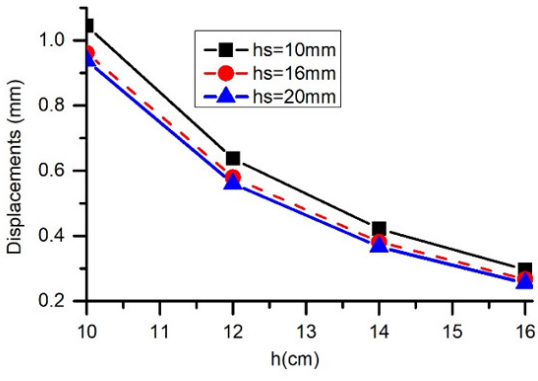

Fig. 3. Displacement of plate with various thicknesses.

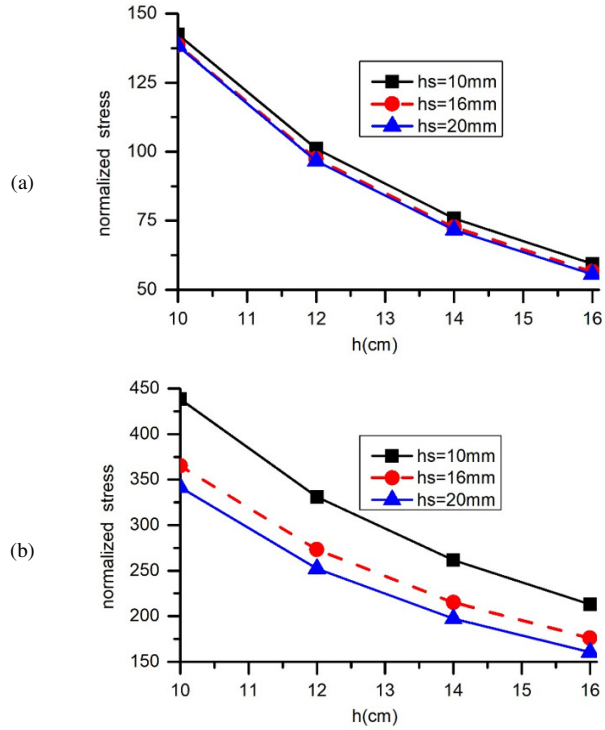

Fig. 4. Normalized srtress σ_x at central plate with various thicknesses: (a) at the top, (b) at the bottom.

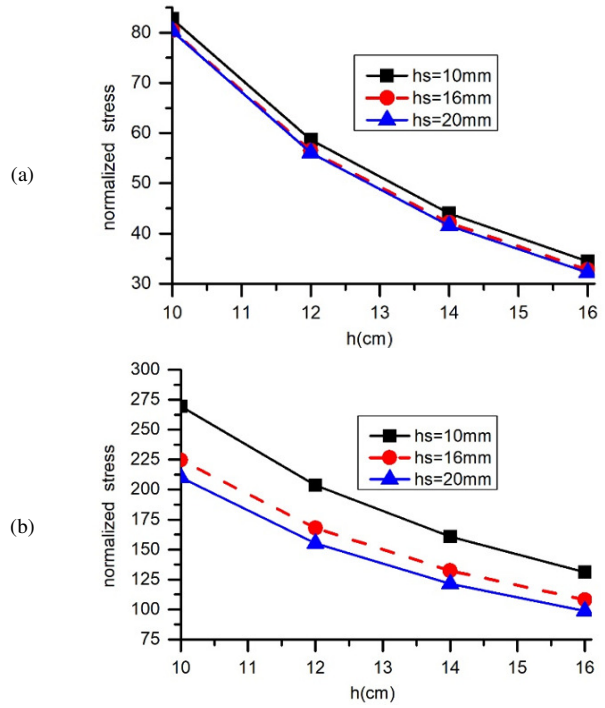

Fig. 5. Normalized srtress σ_y at central plate with various thicknesses: (a) at the top, (b) at the bottom.

It is evident that the plate thickness exerts a notable influence on both displacement and stress. However, when the plate thickness is held constant, the steel plate thickness has a

less significant impact on displacement. Upon increasing the plate thickness to 15 cm, a discrepancy of over 10% between the CPT displacement predictions and the higher-order plate theory is observed.

V. CONCLUSIONS

This research presents the governing equation of the static bending of Steel Concrete Composite (SCC), employing the Classical Plate Theory (CPT) and the Refined Plate Theory (RPT). Analytical solutions were derived for simply supported rectangular plates using the Navier method. The computational results indicate a notable reduction in plate displacement as the plate thickness is increased. Nevertheless, the thickness of the steel plate exerts a relatively limited influence on the plate displacement. The numerical examples demonstrate that when the ratio of the plate thickness to its height exceeds 10, the warping deformation has a considerable impact on the plate displacement. The plate displacement, when shear deformation is taken into account, is in an excess of 10% greater than in the case where shear deformation is not considered.

REFERENCES

[1] J. Singh and A. Kumar, "Vibration and the Buckling Response of Functionally Graded Plates According to a Refined Hyperbolic Shear Deformation Theory," *Mechanics of Composite Materials*, vol. 59, no. 4, pp. 725–742, Sep. 2023, https://doi.org/10.1007/s11029-023-10127-5.

[2] A. W. de Q. R. Reis, R. B. Burgos, and M. F. F. de Oliveira, "Nonlinear Dynamic Analysis of Plates Subjected to Explosive Loads," *Latin American Journal of Solids and Structures*, vol. 19, Jan. 2022, Art. no. e422, https://doi.org/10.1590/1679-78256706.

[3] L. Kurpa, T. Shmatko, and A. Linnik, "Buckling Analysis of Functionally Graded Sandwich Plates Resting on an Elastic Foundation and Subjected to a Nonuniform Loading," *Mechanics of Composite Materials*, vol. 59, no. 4, pp. 645–658, Sep. 2023, https://doi.org/10.1007/s11029-023-10122-w.

[4] N. T. Hiep, D. S. Dan, N. D. Diem, and D. N. Tien, "NURBS-based Isogeometric Analysis and Refined Plate Theory Application on a Functionally Graded Plate Subjected to Random Loads," *Engineering, Technology & Applied Science Research*, vol. 13, no. 2, pp. 10243–10248, Apr. 2023, https://doi.org/10.48084/etasr.5478.

[5] R. Abdikarimov, M. Amabili, N. Vatin, and B. Eshmatov, "Nonlinear vibrations and dynamic stability of viscoelastic anisotropic fiber reinforced plates," *Magazine of Civil Engineering*, vol. 118, no. 2, 2023, Art. no. 11811, https://doi.org/10.34910/MCE.118.11.

[6] D. T. Thuy, L. N. Ngoc, D. N. Tien, and H. V. Thanh, "An Analytical Solution for the Dynamics of a Functionally Graded Plate resting on Viscoelastic Foundation," *Engineering, Technology & Applied Science Research*, vol. 13, no. 1, pp. 9926–9931, Feb. 2023, https://doi.org/10.48084/etasr.5420.

[7] H. D. Ta and P.-C. Nguyen, "Perturbation based stochastic isogeometric analysis for bending of functionally graded plates with the randomness of elastic modulus," *Latin American Journal of Solids and Structures*, vol. 17, no. 7, Sep. 2020, Art. no. e306, https://doi.org/10.1590/1679-78256066.

[8] A. Babiker, Y. M. Abbas, M. I. Khan, and J. M. Khatib, "Kinetic response of reinforced concrete slabs to high-velocity projectile impact-robust numerical and statistical driven modeling techniques," *Latin American Journal of Solids and Structures*, vol. 21, no. 3, Feb. 2024, Art. no. e536, https://doi.org/10.1590/1679-78258009.

[9] T. T. Nguyen, T. S. Le, T. T. Tran, and Q. H. Pham, "Buckling analysis of functionally graded porous variable thickness plates resting on Pasternak foundation using ES-MITC3," *Latin American Journal of Solids and Structures*, vol. 21, no. 2, Jan. 2024, Art. no. e524, https://doi.org/10.1590/1679-78257886.

[10] M. A. Eltaher, O. A. Aleryani, A. Melaibari, and A. A. Abdelrahman, "Bending and Vibration of a Bio-Inspired Bouligand Composite Plate Using the Finite-Element Method," *Mechanics of Composite Materials*, vol. 59, no. 6, pp. 1199–1216, Jan. 2024, https://doi.org/10.1007/s11029-023-10166-y.

[11] P. B. Thang and L. V. Anh, "Structural analysis of steel-concrete composite beam bridges utilizing the shear connection model," *Transport and Communications Science Journal*, vol. 72, no. 7, pp. 811–823, Sep. 2021, https://doi.org/doi.org/10.47869/tcsj.72.7.4.

[12] T. D. Nhiem, *Report on solutions, design and construction techniques to strengthen Thang Long bridge deck. Technological solutions to repair and strengthen Thang Long bridge deck*. Ha Noi, Vietnam: University of Transport and Communications, 2020

[13] X.-B. Luu and S.-K. Kim, "Finite Element Modeling of Interface Behavior between Normal Concrete and Ultra-High Performance Fiber-Reinforced Concrete," *Buildings*, vol. 13, no. 4, Apr. 2023. Art. no. 950, https://doi.org/10.3390/buildings13040950.

[14] N. H. Cuong and N. D. Quang, "Experimental study on flexural behavior of prestressed and non-prestressed textile reinforced concrete plates," *Transport and Communications Science Journal*, vol. 71, no. 1, pp. 37–45, Jan. 2020, https://doi.org/10.25073/tcsj.71.1.5.

[15] D. L. Nguyen, H. V. Le, T. B. N. Vu, V. T. Nguyen, and N. T. Tran, "Evaluating fracture characteristics of ultra-high-performance fiber-reinforced concrete in flexure and tension with size impact," *Construction and Building Materials*, vol. 382, Jun. 2023, Art. no. 131224, https://doi.org/10.1016/j.conbuildmat.2023.131224.

[16] H. D. Ta and H. C. Noh, "Analytical solution for the dynamic response of functionally graded rectangular plates resting on elastic foundation using a refined plate theory," *Applied Mathematical Modelling*, vol. 39, no. 20, pp. 6243–6257, Oct. 2015, https://doi.org/10.1016/j.apm.2015.01.062.

[17] P. M. Phuc, "Using phase field and third-order shear deformation theory to study the effect of cracks on free vibration of rectangular plates with varying thickness," *Transport and Communications Science Journal*, vol. 71, no. 7, pp. 853–867, Sep. 2020, https://doi.org/doi.org/10.47869/tcsj.71.7.10.

[18] Q. H. Pham, T. T. Tran, and P. C. Nguyen, "Dynamic response of functionally graded porous-core sandwich plates subjected to blast load using ES-MITC3 element," *Composite Structures*, vol. 309, Apr. 2023, Art. no. 116722, https://doi.org/10.1016/j.compstruct.2023.116722.

[19] T. D. Hien, N. D. Hung, N. T. Hiep, G. V. Tan, and N. V. Thuan, "Finite Element Analysis of a Continuous Sandwich Beam resting on Elastic Support and Subjected to Two Degree of Freedom Sprung Vehicles," *Engineering, Technology & Applied Science Research*, vol. 13, no. 2, pp. 10310–10315, Apr. 2023, https://doi.org/10.48084/etasr.5464.

[20] B. Pu, X. Wang, W. Li, and J. Feng, "Analytical Model Formulation of Steel Plate Reinforced Concrete Walls against Hard Projectile Impact," *Applied Sciences*, vol. 12, no. 1, Jan. 2022, Art. no. 518, https://doi.org/10.3390/app12010518.

[21] A. M. Olajumoke and M. Dundu, "Dynamic performance of steel plate-strengthened reinforced concrete slabs in bending," in *Advances in Engineering Materials, Structures and Systems: Innovations, Mechanics and Applications*, 1st ed., London: England & Wales, 2019.

[22] M. Ghalehnovi, M. Yousefi, A. Karimipour, J. de Brito, and M. Norooziyan, "Investigation of the Behaviour of Steel-Concrete-Steel Sandwich Slabs with Bi-Directional Corrugated-Strip Connectors," *Applied Sciences*, vol. 10, no. 23, Jan. 2020, Art. no. 8647, https://doi.org/10.3390/app10238647.

[23] M. Zhou, J. Wang, J. Nie, and Q. Yue, "Experimental study and model of steel plate concrete composite members under tension," *Journal of Constructional Steel Research*, vol. 185, Oct. 2021, Art. no. 106818, https://doi.org/10.1016/j.jcsr.2021.106818.

[24] R. P. Shimpi and H. G. Patel, "A two variable refined plate theory for orthotropic plate analysis," *International Journal of Solids and Structures*, vol. 43, no. 22, pp. 6783–6799, Nov. 2006, https://doi.org/10.1016/j.ijsolstr.2006.02.007.

[25] J. N. Reddy, *Mechanics of Laminated Composite Plates and Shells: Theory and Analysis*, 2nd ed. Boca Raton, Florida, United States: CRC Press, 2003.